HHS Public Access

Author manuscript

Arterioscler Thromb Vasc Biol. Author manuscript; available in PMC 2021 May 01.

Published in final edited form as:

Arterioscler Thromb Vasc Biol. 2020 May ; 40(5): 1311–1324. doi:10.1161/ATVBAHA.120.314033.

PI(4,5)P_2 regulates plasma cholesterol through LDL receptor lysosomal degradation

Yuanyuan Qin[1], **Flora Ting**[1], **Mee J Kim**[2], **Jacob Strelnikov**[2], **Joseph Harmon**[2], **Feng Gao**[2], **Andrea Dose**[2], **Ba-Bie Teng**[3], **M. Amir Alipour**[4], **Zemin Yao**[4], **Rosanne Crooke**[5], **Ronald M. Krauss**[1], **Marisa W. Medina**[1]

[1]Department of Pediatrics, University of California San Francisco, Oakland, CA 94609

[2]Children's Hospital Oakland Research Institute, Oakland, CA 94609

[3]Center for Human Genetics, University of Texas Health Science Center, Houston, TX 77030

[4]Department of Biochemistry, Microbiology and Immunology, Ottawa Institute of Systems Biology, University of Ottawa, Ontario, Canada, K1H8M5

[5]Ionis Pharmaceuticals, 2855 Gazelle Court, Carlsbad, CA 92010

Abstract

Objective: Transmembrane protein 55B (TMEM55B) is a phosphatidylinositol-(4,5)-bisphosphate (PI(4,5)P_2) phosphatase that regulates cellular cholesterol, modulates LDL receptor (LDLR) decay and lysosome function. We tested the effects of *Tmem55b* knockdown on plasma lipids in mice, and assessed the roles of LDLR lysosomal degradation and change in (PI(4,5)P_2) in mediating these effects.

Approach and Results: Western diet-fed C57BL/6J mice were treated with antisense oligonucleotides against *Tmem55b* or a non-targeting control for 3–4 weeks. Hepatic *Tmem55b* transcript and protein levels were reduced by ~70%, and plasma non-HDL cholesterol was increased ~1.8-fold ($p<0.0001$). Immunoblot analysis of FPLC fractions revealed enrichment of apoE-containing particles in the LDL size range. In contrast, *Tmem55b* knockdown had no effect on plasma cholesterol in *Ldlr*$^{-/-}$ mice. In primary hepatocytes and liver tissues from *Tmem55b* knockdown mice, there was decreased LDLR protein. In the hepatocytes there were increased lysosome staining and increased LDLR-lysosome colocalization. Impairment of lysosome function (incubation with NH_4Cl or knockdown of the lysosomal proteins *LAMP1* or *RAB7*) abolished the effect of *TMEM55B* knockdown on LDLR in HepG2 cells. Colocalization of the recycling endosome marker RAB11 with LDLR in HepG2 cells was reduced by 50% upon *TMEM55B* knockdown. Finally, knockdown increased hepatic PI(4,5)P_2 levels *in vivo* and in HepG2 cells, while *TMEM55B* overexpression *in vitro* decreased PI(4,5)P_2. *TMEM55B* knockdown decreased, while overexpression increased, LDL uptake in HepG2 cells. Notably, *TMEM55B* overexpression effect was reversed by incubation with PI(4,5)P_2.

Address correspondence to: Dr. Marisa W. Medina, Department of Pediatrics, University of California, San Francisco, 5700 Martin Luther King Jr. Way, Oakland, CA 94609, Tel: 510-450-7977, marisa.medina@ucsf.edu.

DISCLOSURES

None.

Conclusion: These findings indicate a role for TMEM55B in regulating plasma cholesterol levels by affecting PI(4,5)P_2 mediated LDLR lysosomal degradation.

Graphical Abstract

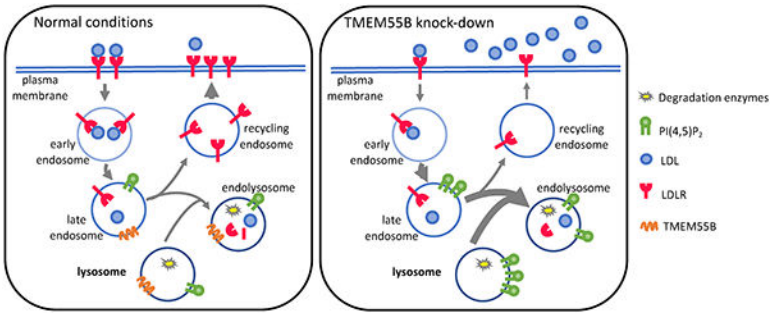

Keywords

cholesterol; lipoprotein; phosphatase; low-density lipoprotein receptor; lysosome

Subject codes:

Lipids and Cholesterol

INTRODUCTION

Hepatic low-density lipoprotein receptors (LDLRs), play an important role in determining plasma cholesterol levels and the risk for cardiovascular disease (CVD). Upon binding of plasma LDLs, cell surface LDLRs are internalized and transported to endosomes, where low pH causes LDLR-LDL dissociation[1]. LDLRs are then either transported to lysosomes for degradation or recycled to the cell surface for reuse[2]. The potential for reducing CVD risk by inhibiting LDLR degradation has been demonstrated by the clinical efficacy of inhibitors of PCSK9, a protein that targets LDLR protein to the lysosome for decay[3].

Recently our laboratory identified transmembrane protein 55B (TMEM55B) as a novel regulator of LDLR decay[4, 5]. We found that *TMEM55B* knockdown in human hepatoma cells decreased intracellular cholesterol level, reduced total LDLR protein level, impaired LDL uptake, and increased LDLR protein degradation[6]. TMEM55B was originally reported to be a late endosome/lysosome-localized type I phosphatase that converts phosphatidylinositol-(4,5)-bisphosphate [PI(4,5)P_2] to PI5P[7]. PI(4,5)P_2 has been shown to impact many subcellular processes including endocytosis, endosome trafficking, and importantly, lysosome function and reformation[8, 9]. Inhibition of lysosome activity increases cell surface LDLRs[10], suggesting that PI(4,5)P_2 may modulate LDLR through its effect on LDLR lysosomal decay. Notably, other PI(4,5)P_2 phosphatases (e.g. Lowe oculocerebrorenal syndrome protein (OCRL), also known as INPP5F) and kinases have been reported to impact trafficking and degradation of the epidermal growth factor receptor and the transferrin receptor, which are recycled and degraded in a manner similar to LDLR[11–13].

Based on the effects of TMEM55B on LDLR *in vitro*, we sought to establish the physiological impact of PI(4,5)P_2 on lipoprotein metabolism *in vivo* using murine models, and to test whether these effects are dependent on LDLR lysosomal decay. Here we report that *Tmem55b* knockdown increases plasma non-HDL cholesterol through an LDLR-dependent mechanism involving PI(4,5)P_2-mediated lysosomal degradation and reduced recycling of LDLRs to the plasma membrane.

MATERIALS AND METHODS

The data that support the findings of this study are available from the corresponding author upon reasonable request.

Animal studies

Animal studies were performed with the approval and in accordance with the guidelines of the Institutional Animal Care and Use Committee at the Children's Hospital Oakland Research Institute (CHORI). Animals were cared for according to the recommendations of the Panel on Euthanasia of the American Veterinary Medical Association. The animal facility is Association for Assessment and Accreditation of Laboratory Animal Care (AAALAC) approved and is responsible for the health and husbandry of animals. Animal studies comply with the Animal Research: Reporting of In Vivo Experiments (ARRIVE) guidelines. Mice were housed in a climate-controlled Department of Laboratory Animal Medicine facility with a 12-hour light-dark cycle and ad libitum access to food and water.

ASO in vivo studies

C57BL/6J, and Ldlr$^{-/-}$ male and female mice were purchased from the Jackson Laboratory (Bar Harbor, ME). Lowe Syndrome mice and PIKFyve$^{+/-}$ mice were generously gifted by Dr. Robert Nussbaum at University of California, San Francisco, and Dr. Lois Weisman at University of Michigan, Ann Arbor, respectively. All mice were i.p. injected with antisense oligonucleotides (ASO) targeting *Tmem55b* or a non-targeting ASO (Ionis Pharmaceuticals) at a dose of 25 mg/ kg body weight/week and fed Western diet (43%fat, 0.2% cholesterol, Harlan Laboratories, Madison, WI) starting at 6–7 weeks old. The ASOs were designed, synthesized, screened, and purified by Ionis Pharmaceuticals (Carlsbad, CA). The two ASOs complementary to murine Tmem55b were: 5'-ATGTTCGTGTCTACTC-3' (T1 ASO); and 5'- AATCTCAGTACTGTA-3' (T2 ASO). In addition, a set of animals were treated with a non-targeting control ASO (NTC ASO).

Body weight was measured prior to the first ASO injection, and weekly until sacrifice. After 3–4 weeks, mice were fasted for 4 hours, and anesthetized with isoflurane (Henry Schein, Melville NY). Blood was collected via cardiac puncture and plasma was separated from other blood components by centrifugation at 850× g for 15 min at 4 °C. Liver, skeletal muscle, and adipose tissues were collected and flash frozen in liquid nitrogen. Gross body composition including lean mass and fat mass was measured using the PixiMus dual energy X-ray absorptiometry (DEXA) device at the UC Davis Mouse Metabolic Phenotyping Center after mice were treated with ASO and fed Western diet for 15 weeks. Percentage of fat mass was calculated as percent fat mass over total body weight[14].

Plasma lipid and lipoprotein analyses

Total cholesterol (TC), HDLc and triglycerides were measured by enzymatic end-point measurements using enzyme reagent kits (Ciba-Corning Diagnostics Corporation) in an AMS Liasys 330 Clinical Chemistry Analyzer[15]. Non-HDLc was calculated by subtraction of HDLc from TC. Lipoprotein particle concentrations were measured by gas-phase electrophoresis (ion mobility)[16]. Briefly, this method employs an ion separation/particle detector system that separates ions by size and which can count lipoprotein particles over a wide range of sizes. Complete details of this technique had been previously described[17]. Plasma (200 μl) was separated by fast protein liquid chromatography (FPLC) on two Superose 6 columns (Amersham Biosciences, Piscataway, NJ). Fractions (0.5 ml each) were eluted using 150 mM NaCl, 1 mM EDTA and 0.02% NaN3 pH 8.2 to separate VLDL, LDL, and HDL[18]. Total cholesterol and TG concentrations in both plasma and each FPLC fraction were determined using the Cholesterol E and the L-Type Triglyceride M kits (Wako Chemicals, Richmond, VA), respectively.

Quantitative real-time PCR

RNA was extracted from liver and reverse transcribed into cDNA as previously described[5]. All assays were carried out in triplicate using 50ng cDNA in an ABI PRISM 7900 Sequence Detection System using the qPCR assays. Grubb's test for outliers was used to identify statistical outliers from the triplicate values. The real-time PCR results were normalized to *Clptm* as an internal control.

Western blot analyses

TMEM55B protein expression was measured by immunoblotting as previously described[19]. Briefly, liver tissues were homogenized in CelLytic M (Sigma-Aldrich) lysis buffer with protease Inhibitor Cocktail (Thermo Fisher Scientific), centrifuged for 15 min at x16,000g at 4°C, and the supernatants were collected. Samples were eluted with Laemmli buffer and denatured at 95°C for 5 min before loading to 8% or 4–20% Tris-Glycine gels (Thermo Fisher Scientific). After running on PowerEaseTM 90W Power Supply (115 VAC) (Thermo Fisher Scientific) at a constant 150 voltage for 1.5 h, samples were transferred to a Polyvinylidene difluoride (PVDF) membrane, and incubated with anti-TMEM55B or anti-GAPDH antibody at 4°C overnight, washed 3 times and incubated with secondary antibody for 1 h at room temperature. Enhanced chemiluminescence substrate (Thermo Fisher Scientific) was used for protein detection. Quantitative analysis of protein bands was performed using Image J (NIH, Bethesda, MD).

Mouse plasma fractions after FPLC were diluted with PBS at 1:5, and 10 μl of each fraction was loaded on a ProSieve-50 6% or 10% gel (FMC BioProducts, Rockland, ME). After electrophoresis, gels were incubated with anti-mouse apoB (ab20737, Abcam, Cambridge, MA), anti-mouse apoE, or anti-mouse apoAI (generously gifted by B. Ishida, UCSF). Protein band intensity was detected using an Odyssey Infrared Imaging system (Li-COR, Lincoln, NE). Quantitative analysis of protein bands was performed using Image J.

Hepatic lipid measurements

Liver tissues were homogenized with GentleMacs (Miltenyi Biotec Inc. Auburn, CA) and netural lipids extracted with chloroform:methanol (2:1) according to the Folch method[20]. Chloroform extracts were dried under N_2 gas and resuspended in 200 μl isopropyl alcohol containing 10% Triton X-100. TAG, TC, and free cholesterol were measured using the L-Type TG M kit, Cholesterol E kit, free cholesterol E kits.

PI(4,5)P_2 and PCSK9 ELISA

PI(4,5)P_2 levels were quantified by using the PI(4,5)P_2 Mass ELISA kit from Echelon Bioscience (Salt Lake City, UT). Briefly, the acidic lipid was extracted from liver lysates with chloroform: methanol: 12N HCl (40:80:1)[21]. Chloroform and 0.1N HCl was added to the supernatant. The bottom organic phase was collected, dried, suspended in PBS with 0.25% protein Stablizer (K-GS01, Echelon Biosceience), and subjected to the PI(4,5)P_2 Mass ELISA assay according to the Echelon protocol. Plasma PCSK9 levels were quantified using the Mouse Proprotein Convertase 9/PCSK9 Quantikine ELISA Kit (MPC900) from R&D Systerms (Minneapolis, MN). Mouse plasma was diluted 200-fold with Calibrator Dilutent RD5–26 (895525, R&D Systems) prior to PCSK9 quantification.

Cell culture, transfection and treatments

HepG2 cells were grown at 37°C and 5% CO_2 in Eagle's Minimum Essential Medium (EMEM) (ATCC, Manassas, VA) or high-glucose Dulbecco's Modified Eagle's Medium (DMEM) (McArdle cells) (ATCC) supplemented with 10% FBS (HyClone, Logan, Utah), 500 U/mL penicillin/streptomycin, and 2 nmol/L GlutaMAX (Invitrogen). *TMEM55B*, *LAMP1*, *RAB7*, and *LDLRAP1* knockdown were achieved by transfection of 80,000 HepG2 cells/well in 12-well plates with siRNAs (Life Technologies) targeting *TMEM55B* (S40499), *LAMP1* (S8082), *RAB7* (S1552), *LDLRAP1* (23202) according to the manufacturer's protocol and compared to cells transfected with a scrambled control siRNA. For double knockdown, *TMEM55B* and *LAMP1*, *TMEM55B* and *RAB7*, or *TMEM55B* and *LDLRAP1* siRNAs were co-transfected into the HepG2 cells. Cellular phenotypes were quantified 36 hours post-transfection. For *TMEM5B* overexpression, 80,000 HepG2 cells/well were plated in a 12-well plate, and transfected with control GFP or *TMEM55B*-GFP with Amaxa™ Nucleofector™ II from Lonza (Basel, Switzerland). Primary hepatocytes were isolated from T2-ASO and NTC-ASO treated 12-week-old male mice at the UCSF Liver Center using the standard collagenase method[22].

Immunofluorescence staining and confocal microscopy

siRNA transfected cells and primary hepatocytes were seeded to cover glass slides. After 12 hr, cells were incubated with 10 mM NH_4Cl (09718, Sigma-Aldrich) or sham buffer at 37°C for 24 hr. Cells were then washed with PBS and fixed with 4% paraformaldehyde in PBS for 10 min at room temperature. For lysosome staining with LysoTracker (L7528, Life Technologies, CA), cells were treated with 75nM LysoTracker DND 99 probes for 2 hr in the cell incubator before fixation. Cells were permeabilized in 0.25% Triton-100 in PBS for 10 min at room temperature. After washing with PBS, cells were treated with 1% BSA, 22.52 mg/mL glycine in PBST (PBS+ 0.1% Tween 20) for 30 min to block nonspecific

antibody binding, and incubated overnight at 4°C with primary antibodies [i.e. LDLR, LAMP1, RAB7, RAB11, TFR, LRP1, PI(4,5)P_2] or control IgG diluted in 0.1% PBST. After 3 washes with PBS, cells were incubated for 1 hr at room temperature with secondary antibodies diluted in 0.1% PBST, and subsequently washed 3 times with PBS.

The samples were examined under a Zeiss LSM 710 confocal laser-scanning microscope equipped with an X63 oil-immersion objective. To perform quantitative image analysis, 15–35 randomly chosen fields that included 1–5 cells each were scanned using the same setting parameters (i.e., laser power and detector amplification) below pixel saturation. The mean intensity per field was determined using the histogram function in the Zeiss LSM 710 Software, and all of the pixel values above background levels (established from the control IgG treated cells) were quantified. Each experiment was repeated at least three times, and representative images were shown.

To quantify the levels of colocalization of LAMP1/LDLR and RAB11/LDLR, 15–35 randomly chosen fields that included 1–5 cells each were scanned and analyzed in Carl Zeiss software AIM using Pearson's correlation coefficients. All imaging parameters and analyzing settings remained the same for all data acquisition within one experiment.

Flow cytometry

To quantify LDL uptake, HepG2 cells were transfected with *TMEM55B* over-expression (OE) or empty-vector (EV) plasmids for 48hr, and incubated with PI(4,5)P_2 (Y-P045) or control liposomes (Y-0000) (Echelon Bioscience. Salt Lake City, UT). They were then exposed to 10 μg/ml fluorescently labelled Dil-LDL (L3482, Invitrogen Carlsbad, C) for 3–4 h at 37°C, washed twice with ice-cold PBS, fixed in 1% formaldehyde, and scraped from the wells. Dil was quantified on the BD FACS Calibur as the median fluorescence values of 10,000 gated events.

Live cell imaging

McArdle cells were plated on 35-mm glass bottom dishes (Ibidi GmbH München, Germany) in DMEM supplemented with FBS (20%) and oleate (0.4 mM) 16 h prior to siRNA transfection. Live cell images were acquired 24 hr after transfection using a Zeiss LSM 780 microscope (Carl Zeiss) equipped with a stage heated to 37°C in a chamber containing 5 % CO2 (v/v)/95 % (v/v) air. Images were captured at the frame-rate of 30 frame/sec using a 60X.1.4 objective and numerical aperture with the laser selected to the dye specificity.

Membrane fraction isolation

HepG2 cells were treated with lipoprotein depleted-serum and 2μM simvastatin for 24 hour before being lysed with IP Lysis Buffer (Pierce™ Direct Magnetic IP/Co-IP Kit; Pierce Biotechnology, Rockford, IL) containing protease inhibitors (Halt™ Protease Inhibitor Cocktail; Thermo Scientific, Waltham, MA). The membrane fraction was isolated as described in Hashimoto *et al.*[23]. Briefly, the cells were homogenized in a solution containing 20 mmol/L HEPES-NaOH (pH 7.5), 0.25 mol/L sucrose, 1 mmol/L Na3 VO4, 25 mmol/L NaF, aprotinin (10 μg/ml), leupeptin (10 μg/ml), 10 μmol/L MG132 and 1 mmol/L PMSF. The homogenate was centrifuged at 1,000 X g for 5 min at 4°C to remove nuclei and

nondisrupted cells, and the resulting supernatant was centrifuged at 100,000 X g for 1 hr at 4°C to isolate a membrane pellet. The pellet was solubilized by sonication, and the insoluble material was removed by centrifugation at 20,400 X g for 15 min at 4°C.

Co-immunoprecipitation

Cells were collected, washed with TBS, and lysed in IP Lysis Buffer (Pierce™ Direct Magnetic IP/Co-IP Kit; Pierce Biotechnology, Rockford, IL) containing protease inhibitors (Halt™ Protease Inhibitor Cocktail; Thermo Scientific, Waltham, MA) by incubating on ice for 30 min with gentle vortexing every 10 min. The cell lysate was centrifuged at 13,000 g for 10 min. The supernatant was collected and protein concentration was measured by Bradford protein assay (Bio-Rad, Hercules, CA). TMEM55B proteins were isolated via magnetic beads coupled to anti-TMEM55B antibody (Proteintech, Rosemont, IL) as described[24]. Briefly, anti-TMEM55B antibody (5 μg/reaction) was first coupled with Pierce NHS-Activated Magnetic Beads for 60 minutes at room temperature. The beads were then washed twice and quenched with Quenching Buffer (Pierce Biotechnology, Rockford, IL). After overnight incubation of cell lysates with beads at 4°C, the beads were washed twice with IP Lysis Buffer before protein elution with Elution Buffer for 5 minutes at room temperature. A negative control antibody (isotope IgG) was used to assess nonspecific binding. Eluted samples were analyzed by immunoblotting as described in Western blot analyses.

Statistics

For *ex vivo* and *in vitro* experiments, representative results are shown. At least 3 experiments were conducted with 3–6 replicates per assay, with specific replicate numbers indicated in figure legends. All data are shown as mean ± standard error of the mean. Normality of data was tested with the D'Agostino-Pearson normality test. Homogeneity of variance was tested with the Bartlett's test or F test. Continuous variables for two groups were compared using Student's t-tests. Continuous variables for more than two groups were compared using one-way analysis of variance (ANOVA) with Tukey's post hoc test. Analyses were performed using GraphPad Prism 7 software (GraphPad Software, Inc. La Jolla, CA, USA). P-values <0.05 were considered statistically significant.

RESULTS

Knockdown of Tmem55b increases plasma non-HDL cholesterol in C57BL6J mice

To determine if Tmem55b modulates cholesterol metabolism *in vivo*, we tested the effect of hepatic knockdown using two antisense oligonucleotides (ASOs T1 and T2) targeting *Tmem55b*. After 4 weeks of weekly ASO injections, hepatic *Tmem55b* transcript and protein levels in Western diet-fed male C57BL/6J mice were reduced by 71% and 56% (T1) and 61%, and 70% (T2), respectively, compared to animals treated with a non-targeting control ASO (NTC) (Fig. 1A, 1B). In contrast, there were no changes in expression of hepatic *Tmem55a*, a type II PI(4,5)P_2 phosphatase with sequence similarities to *Tmem55b*, between T1, T2 and NTC treated animals, (Fig. SIA). Although ASOs have been reported to mainly target the liver[25], we also found that both T1 and T2 ASO treatment significantly decreased *Tmem55b* transcript levels in muscle and adipose tissue compared to NTC

treatment (Fig. SIB, SIC). In Western diet-fed female mice, simultaneous administration of T1 and T2 (T1+T2) ASO reduced hepatic *Tmem55b* transcript (71%) and protein (53%) levels compared to NTC (Fig. 1C, 1D). *Tmem55b* knockdown did not alter whole body, liver or gonadal adipose weights (Fig. 2A, 2C, SIIA–D) in either male or female mice, or measures of whole-body fat mass, lean mass or adiposity as quantified by DEXA (Fig. SIIIA–C).

T1 or T2 ASO treated Western diet-fed male mice had increased plasma total cholesterol (1.3-fold, p=0.016; 1.5-fold, p<0.0001), HDL cholesterol (1.2-fold, p=0.0071; 1.3-fold, p=0.0017), and non-HDL cholesterol (1.5-fold, p<0.0001; 1.8-fold, p<0.0001), n=9–10 (Fig. 2B; Fig. SIVA). There were no differences in any of these measurements between T1, T2, and T1+T2 ASO treatments (Fig. SIVB). In Western diet-fed female mice, *Tmem55b* knockdown increased TC (1.3-fold, p=0.0009) and non-HDLc (1.6-fold, p<0.0001), with a trend of increased HDLc (1.1-fold, p=0.08) observed between T1+T2 and NTC ASO treated animals, n=6 (Fig. 2D; Fig. SIVC). *Tmem55b* knockdown did not alter plasma triglyceride levels in either male or female mice (Fig. 2B, 2D) nor did it change hepatic total cholesterol, free cholesterol or triglyceride levels, Fig. SIVD.

Tmem55b knockdown increases apoE-containing lipoproteins

To further define the impact of *Tmem55b* knockdown on plasma lipoproteins, we analyzed levels of cholesterol and apolipoproteins (ApoB100, ApoB48, ApoE and ApoA1) in fast protein liquid chromatography (FPLC) fractionated plasma. T1+T2 ASO treated female mice had increased plasma cholesterol in the LDL size range (Fig. 3A). Although there was no change in either ApoB100, B48 or ApoA1 in these fractions, ApoE was increased between 1.6–8.0 fold across the fractions (Fig. 3B, 3C). Similarly in male mice, both T1 and T2 ASO treatment led to increased cholesterol levels in LDL fractions from FPLC (Fig. SVA). There were no significant differences in triglyceride content in any of the fractions between *Tmem55b* and NTC ASO mice in either sex (Fig. SVB, SVC).

We also used ion mobility as a highly sensitivity means of determining lipoprotein particle concentrations in plasma independent of their lipid content[16]. This revealed that *Tmem55b* knockdown in both sexes significantly increased lipoprotein levels in the size ranges attributed to small LDL, as well as the region between LDL and HDL, with smaller increases in particles in the size range of very low and intermediate density lipoproteins (VLDL and IDL) (Fig. SVIA, SVIB, SVIIA, SVIIB). We repeated the ion mobility analyses in plasma after treatment with dextran sulfate, which precipitates ApoB and ApoE containing particles[26], and consistent with the increased ApoE identified in the FPLC fractions, found no differences in particle concentrations (Fig. SVIC).

Tmem55b regulates plasma lipids through LDLR

We previously showed that *TMEM55B* knockdown in human hepatoma cell lines reduces LDLR protein levels[5]. To confirm this effect *in vivo*, we quantified changes in hepatic LDLR protein levels in Western diet-fed male C57BL/6J mice after 4 weeks of T1 or T2 ASO injections and found a 48% reduction in LDLR in the T2 treated animals (p<0.05) (Fig. SX). A similar, non-statistically significant trend of reduced LDLR in the T1 treated animals

was also observed (Fig. SX). We also isolated primary hepatocytes from T2 ASO (which had more potent effects than T1 ASO in elevating plasma cholesterol levels) and NTC ASO treated mice. We found that *Tmem55b* knockdown reduced LDLR protein levels by 10% ($p<0.05$, Fig. 5A), a magnitude of effect consistent with our *in vitro* studies[5]. Conditions of reduced LDLR are known to cause accumulation of plasma PCSK9[27]. Consistent with the reduced LDLR protein levels, we also found higher plasma PCSK9 in the T2 vs. NTC ASO treated mice ($p<0.05$, n=3. Fig. SVIII). Finally, to test whether the increase in plasma lipids after *Tmem55b* knockdown was mediated by LDLR, we treated Western diet-fed male and female $Ldlr^{-/-}$ mice with either combined T1+T2 or NTC ASOs weekly. After four weeks *Tmem55b* mRNA was reduced by 85% and 62%, and TMEM55B protein by 88% and 78% in males and females, respectively, (Fig. 4A, 4B, 4D, 4E). Importantly, no statistically significant differences in plasma lipid levels or lipoprotein particle concentrations were observed between *Tmem55b* knockdown and NTC mice in either sex (Fig. 4C, 4F, SIXA–D).

TMEM55B effects on cellular LDLR requires lysosome activity

We previously reported that *TMEM55B* knockdown in human hepatoma cell lines alters LDLR protein decay and cell surface LDLR protein levels[5]. TMEM55B is localized to the late endosome and lysosome[7], and has been shown to impact lysosome function[23, 28]. Thus we hypothesized that TMEM55B regulation of LDLR may be mediated by effects on lysosomal activity. In primary hepatocytes from T2 ASO treated mice, lysosomal associated protein1 (LAMP1), a lysosome structural protein, was significantly increased compared to hepatocytes from NTC ASO treated mice ($p<0.001$, Fig. 5A). Importantly, *Tmem55b* knockdown led to a modest but statistically significant increase in LDLR and LAMP1 colocalization (Fig. 5A). In HepG2 cells treated with a *TMEM55B* vs. control (Scr) siRNA there were consistent effects: reduced LDLR protein, increased lysosome staining (both LAMP1 levels and LysoTracker) and increased LDLR-LAMP1 colocalization (Fig. 5B). In both primary hepatocytes and HepG2 cells, IgG from the same species as the 1° antibody was used as the negative control (Fig. SXIA, SXIB).

LDLR decay typically occurs after internalization, when LDLRs from the cell surface can be delivered to the lysosome for degradation or recycled back to the cell surface[29]. However, it is also possible that newly synthesized LDLR is subject to decay. To distinguish between these possibilities, we used siRNA to knockdown the LDLR adaptor protein 1 (LDLRAP1, also named autosomal recessive hypercholesterolemia protein [ARH]), which is required for LDLR endocytosis[30]. Upon *LDLRAP1* knockdown, *TMEM55B* knockdown did not affect LDLR protein levels (Fig. SXIIA, SXIIB), indicating that TMEM55B modulates LDLR decay after its internalization.

Lysosome activity is dependent on its position within the cell[31, 32]. Thus, to test whether TMEM55B impacts lysosome position (in addition to levels), we treated McArdle cells (a rat hepatoma cell line) with oleic acid, which stimulates fatty acid flux through lysosomes. *Tmem55b* knockdown led to more punctate and larger lysosomes which congregated compared to findings in NTC siRNA treated cells, (Fig. 5C, Supplementary Movie 1, 2). We next tested the effects of *TMEM55B* knockdown on LDLR levels under three conditions of

impaired lysosome function in HepG2 cells: i) treatment with NH_4Cl, which prevents acidification of intracellular vesicles, leading to dysfunction of the lysosome hydrolytic enzymes[33], ii) knockdown of LAMP1, or iii) knockdown of Rab7, a late endosome/lysosome protein. In all three conditions, no changes in LDLR levels were observed upon *TMEM55B* knockdown (Fig. 5D, 5E). To confirm that reduced LDLR levels were not due to a reduction in recycling receptors, we tested for changes in RAB11, a marker of recycling endosomes. There was no change in RAB11 levels upon knockdown, and LDLR-RAB11 colocalization was reduced by 50% (Fig. 5F). Together, these results suggest that TMEM55B regulates LDLR levels through lysosome function.

No evidence of TMEM55B-LDLR binding—To assess whether the effects of TMEM55B on LDLR were attributed to generalized changes in recycling receptor trafficking, we tested the effect of *TMEM55B* knockdown on transferrin receptor (TFR) and LDLR related protein (LRP1), two receptors that undergo a similar endocytic trafficking pathway as LDLR[29]. We found no effect of *Tmem55b* knockdown on either TFR or LRP1 in liver, or primary hepatocytes from mice, or in HepG2 cells(Fig. 6A, 6B, SXIII), consistent with our previous findings[5].

To test whether TMEM55B binds to LDLR, we performed co-immunoprecipitation assays using HepG2 cells transfected with either control GFP or GFP-*TMEM55B*. *TMEM55B*-GFP overexpression was confirmed by immunoblotting in the whole cell lysate (Fig. 6C). Next we performed pull-down with magnetic beads conjugated to anti-TMEM55B, and confirmed TMEM55B protein pull-down versus an IgG negative control (Fig. 6C). In addition, we identified JIP4 in the TMEM55B pull-down as a positive control, as this protein has been previously reported to interact with TMEM55B[28] (Fig. 6D). No LDLR band was observed after TMEM55B pull-down (Fig. 6E). We also performed the reverse experiment whereby we increased LDLR expression in HepG2 cells through treatment with lipoprotein-depleted serum (LPDS) and 2μM simvastatin and pulled down LDLR. We found no evidence of an interaction between TMEM55B and LDLR (Fig. SXIVA, SXIVB). A previous proteomic study of TMEM55B in a neuroblastoma cell line reported a possible interaction between TMEM55B and LDLR that was only observed in the membrane fraction[23]. Thus, we isolated the membrane fraction of LPDS and statin treated HepG2 cells and again failed to detected LDLR protein after TMEM55B pull-down (Fig. SXIVC, SXIVD).

Since we found no evidence for TMEM55B-LDLR binding, we next tested whether TMEM55B might modulate LDLR by altering levels of PCSK9, COMMD1 or MYLIP/IDOL, which are well documented regulators of LDLR protein decay[3, 34, 35]. We found no change in hepatic Pcs9k, Commd1 or Mylip/Idol protein levels in T1 or T2 ASO vs. NTC ASO treated male mice (Fig. 6F).

TMEM55B regulates LDLR activity through $PI(4,5)P_2$

TMEM55B was originally reported to be a phosphatase that catalyzes the conversion of $PI(4,5)P_2$ to PI5P[7]. We confirmed that *Tmem55b* knockdown significantly increased $PI(4,5)P_2$ levels by 94% in the livers from T2 versus NTC ASO treated male mice (Fig. 7A).

Using both confocal microscopy and flow cytometry we confirmed that *TMEM55B* knockdown in HepG2 cells significantly increased cellular PI(4,5)P_2 levels (Fig. 7B, 7C), while *TMEM55B* overexpression (OE) decreased PI(4,5)P_2 levels (Fig. 7D, 7E). Consistent with its reported endosome/lysosome localization, we found that *TMEM55B* knockdown increased PI(4,5)P_2 -LAMP1 colocalization in HepG2 cells (Fig. 7B), with opposite effects observed after overexpression (Fig. 7D).

We next tested the effect of PI(4,5)P_2 on LDLR activity in HepG2 cells. We first confirmed that *TMEM55B* OE increased Dil-labeled LDL uptake compared to empty vector (EV) controls (Fig. 7F). Incubation of cells with PI(4,5)P_2-containing liposomes decreased Dil-LDL uptake compared to cells incubated with control liposomes (Fig. 7F). Most importantly, incubation of *TMEM55B*-OE cells with PI(4,5)P_2-containing liposomes decreased Dil-LDL uptake to the level of *TMEM55B*-EV cells (Fig. 7F). Together, these results support the likelihood that TMEM55B regulates LDLR activity and thus plasma non-HDLc through changes in PI(4,5)P_2.

Lastly, to explore whether the changes in plasma lipids upon *Tmem55b* knockdown could be attributed to either increased PI(4,5)P_2 or reduced PI5P, we quantified plasma lipids in two additional mouse models. OCRL is a phosphatase that converts PI(4,5)P_2 to PI4P[11, 36]. Loss of Ocrl has been shown to increase PI(4,5)P_2 levels in ex vivo study[37]. After 4 weeks of Western diet, male *Ocrl* knockout mice had >50% higher non-HDLc than *Ocrl* wildtype littermates (Fig. SXVA). PIKfyve is a phosphoinositide kinase reported to be the major enzyme for generating the PI5P pool[38]. PIKfyve is vital in early embryonic development, and homozygous *PIKfyve*$^{-/-}$ animals are not viable or die shortly after birth[39]. Therefore, we tested whether plasma lipids differed in Western diet-fed *PIKFyve*$^{+/-}$ versus littermate controls and found no differences (Fig. SXVB). Together, these results support the likelihood that the effects of *Tmem55b* knockdown on plasma lipid metabolism are mediated by PI(4,5)P_2.

DISCUSSION

TMEM55B was identified as a novel regulator of cellular cholesterol metabolism through gene expression profiling and *in vitro* studies[5]. Here we report that Tmem55b also regulates plasma cholesterol levels *in vivo*, an effect that is dependent on LDLR, and functions through PI(4,5)P_2-mediated LDLR lysosomal degradation. Phosphatidylinositol 5-phosphate 4-kinase type-2 α (PIP4K2A), which converts PI5P to PI(4,5)P_2, has been reported to regulate intracellular cholesterol transport through PI(4,5)P_2[40]. Plasma membrane PI(4,5)P_2 has been shown to promote ApoA1-ABCA1 mediated lipid efflux from macrophages[21], however, to our knowledge, the present findings are the first to identify a role for phosphatidylinositides in metabolism of non-HDL lipoproteins.

FPLC analysis indicated that ASO-mediated *Tmem55b* knockdown increased cholesterol levels in fractions in the LDL size range, consistent with the results of ion mobility analysis which showed the greatest increases in particle concentrations to be in the size range of small LDL as well as in the size region between LDL and HDL. While there were no detectable changes in apoB in LDL-sized fractions isolated by FPLC, there were significant

increases in apoE content. It is possible that this selective increase in apoE was due to higher levels of apoE-only containing particles, which have been shown to be present in this particle size region[41]. However it should also be noted that Western blot analysis may not be sufficiently sensitive to detect small increases in apoB and/or apoAI levels. The failure of *Tmem55b* knockdown to alter plasma lipids in the $Ldlr^{-/-}$ mouse and the finding that knockdown reduces hepatic LDLR protein suggests that the increases in plasma cholesterol and ApoE containing lipoproteins are, at least in part, LDLR-dependent. Since LDLR can regulate apoB and apoE secretion as well as uptake[42, 43], further study will be required to determine whether one or both of these processes are responsible for the LDLR dependence of the effects of *Tmem55b* knockdown on plasma lipid levels.

Since reduced LDLR was shown to be responsible for the plasma lipid effects of *Tmem55b* knockdown, we next investigated how TMEM55B regulates LDLR. When circulating LDL binds to LDLR, the LDLR-LDL complex is internalized in a clathrin-coated pit on the plasma membrane and trafficked through the endo/lysosomal pathway[45]. In the late endosome where the pH value decreases, LDLR disassociates from LDL, and then is either recycled back to the plasma membrane for reuse, or targeted to the lysosome for decay[46]. We had previously reported that TMEM55B modulates LDLR decay, and very recently TMEM55B was reported to impact lysosome positioning in AREP-19 and HeLa cells[28]. Notably, intracellular localization of lysosomes regulates their ability to interact and fuse with vesicles such as autophagosomes or endosomes[31, 32, 47, 48]. We have shown here that *TMEM55B* knockdown increased LAMP1 and lysotracker staining, stimulated lysosomal clustering, reduced LDLR levels and increased LDLR-lysosome colocalization, with opposite effects observed after *TMEM55B* overexpression. As TMEM55B was unable to alter LDLR levels under conditions of impaired lysosome function, our findings strongly support the conclusion that TMEM55B regulates LDLR through changes in lysosome function.

Given the effect of TMEM55B on the lysosome, it is possible that TMEM55B modulates multiple recycling receptors. However, consistent with our previous studies in HepG2 cells[5], we failed to identify an effect of TMEM55B on either the transferrin receptor or LRP1, which undergo similar cellular trafficking as LDLR[29, 49], in HepG2 cells, primary murine hepatocytes, or mouse liver tissues. These findings demonstrate that TMEM55B regulation of LDLR does not represent a generalized effect on trafficking receptors. However, the mechanism underlying the specificity of TMEM55B regulation of LDLR is unclear as we found no evidence of either direct TMEM55B binding to LDLR, or modulation of other known LDLR-binding proteins (PCSK9, COMMD1 or MYLIP/IDOL). Although, TMEM55B binding to LDLR was reported in isolated cell membranes from neuronal cells[15], we found no such interaction in the cell membrane fraction of a liver-derived cell line (HepG2).

Here we report that *TMEM55B* knockdown leads to increased $PI(4,5)P_2$ levels *in vivo* and *in vitro*. Although $PI(4,5)P_2$ is primarily concentrated at the plasma membrane, it is also found on lysosomes[50]. Lysosomal $PI(4,5)P_2$ serves as an important signaling molecule that regulates traffic from the lysosome[51] and that mediates lysosome reformation after autophagosome fusion[52]. Our finding that the effect of *TMEM55B* overexpression on LDL

uptake is reversed by addition of exogenous $PI(4,5)P_2$ provides evidence that TMEM55B regulates LDLR lysosomal degradation through $PI(4,5)P_2$. This is further supported by the finding that *Ocrl*$^{-/-}$ mice, another mouse model of increased $PI(4,5)P_2$, have higher non-HDL cholesterol than wild type controls.

Although TMEM55B was first identified as a $PI(4,5)P_2$ phosphatase by Ungewickell et al[7], a recent study by Willett *et al* failed to detect $PI(4,5)P_2$ hydrolysis activity of TMEM55B[28]. This discrepancy may be due to differences in the expression system used, as Ungewickell *et al* purified TMEM55B protein in a mammalian system using infected Sf9 cells, while Willett *et al* used a bacterial system with E. coli, leading to potential differences in cellular transport and post translational modifications[53]. Although we did not directly test for phosphatase activity, we found that *TMEM55B* knockdown increased $PI(4,5)P_2$ levels in HepG2 cells and in primary murine hepatocytes, consistent with independent results observed in Raw 264.7 macrophages by Kailash *et al*[21]. The fact that TMEM55B modulates $PI(4,5)P_2$ levels supports our finding that TMEM55B regulation of LDLR is dependent on $PI(4,5)P_2$. Importantly, this dependency may be true whether or not TMEM55B has phosphatase activity as it may modulate $PI(4,5)P_2$ levels through indirect actions (e.g. by recruiting a $PI(4,5)P_2$ phosphatase).

In summary, we have shown that TMEM55B contributes to the dynamic regulation of lysosomal LDLR degradation and recycling, that this effect is mediated by $PI(4,5)P_2$, and that it ultimately impacts plasma non-HDL cholesterol and apoE-enriched lipoprotein levels. Given the importance of LDLR function in the clinical management of elevated plasma cholesterol levels and the prevention of cardiovascular disease, the regulation of LDLR has been extensively studied. However, the present findings highlight that there are as yet unidentified molecular players that impact LDLR regulation and function.

Supplementary Material

Refer to Web version on PubMed Central for supplementary material.

ACKNOWLEDGEMENTS

We gratefully acknowledge the generosity of Dr. Rosa Puertollano for the *TMEM55B*-GFP plasmid, Dr. Robert Nussbaum for Lowe Syndrome (*Ocrl*$^{-/-}$) mice, and Dr. Lois Weisman for PIKFyve$^{+/-}$ mice. We thank Joe Orr, Bahareh Sahami and Sarah King for measuring plasma lipids and lipoproteins, Nick Lee, Lloyd Tripp, Gilbert Nalula and Allison Torres for their assistance in animal studies, Hua Sun of the University of Texas Health Science Center at Houston for processing samples by FPLC, and Dr. Mark Gram of Ionis Pharmaceuticals for the ASOs.

SOURCE OF FUNDING

This work was supported by the NIH (P50 GM115318, R56 HL130288 and R01 HL139902, MM).

Abbreviations:

ABCA1	ATP-binding cassette transporter A1
ARH	Autosomal recessive hypercholesterolemia protein
ASO	Antisense oligonucleotides

CVD	Cardiovascular disease
FPLC	Fast protein liquid chromatography
HDL	High-density lipoprotein receptor
IDL	Intermediate density lipoproteins
INPP5F	Inositol polyphosphate-5-phosphatase F
LAMP1	Lysosome associated membrane protein 1
LDLR	Low-density lipoprotein receptor
LDLRAP1	Low-density lipoprotein receptor adapter protein 1
LRP1	Lipoprotein receptor-related protein 1
OCRL	Lowe oculocerebrorenal syndrome protein
PCSK9	Proprotein convertase subtilisin/kexin type 9
PI(4,5)P_2	Phosphatidylinositol-(4,5)-bisphosphate
PI4P	Phosphatidylinositol 4-phosphate
PIKfyve	Phosphoinositide kinase, FYVE-type zinc finger containing
RAB11	Ras-related protein 11
RAB7	Ras-related protein 7
Scr	Scrambled control
TFR	Transferrin receptor
TG	Triglyceride
TMEM55B	Transmembrane protein 55B
VLDL	Very low-density lipoproteins

REFERENCES

1. Brown MS and Goldstein JL. A receptor-mediated pathway for cholesterol homeostasis. Science. 1986;232:34–47. [PubMed: 3513311]
2. Gao F, Ihn HE, Medina MW and Krauss RM. A common polymorphism in the LDL receptor gene has multiple effects on LDL receptor function. Hum Mol Genet. 2013;22:1424–31. [PubMed: 23297366]
3. Bergeron N, Phan BA, Ding Y, Fong A and Krauss RM. Proprotein convertase subtilisin/kexin type 9 inhibition: a new therapeutic mechanism for reducing cardiovascular disease risk. Circulation. 2015;132:1648–66. [PubMed: 26503748]
4. Krauss RM, Zhu H and Kaddurah-Daouk R. Pharmacometabolomics of statin response. Clin Pharmacol Ther. 2013;94:562–5. [PubMed: 23945822]
5. Medina MW, Bauzon F, Naidoo D, Theusch E, Stevens K, Schilde J, Schubert C, Mangravite LM, Rudel LL, Temel RE, Runz H and Krauss RM. Transmembrane protein 55B is a novel regulator of

cellular cholesterol metabolism. Arterioscler Thromb Vasc Biol. 2014;34:1917–23. [PubMed: 25035345]

6. Lo Surdo P, Bottomley MJ, Calzetta A, Settembre EC, Cirillo A, Pandit S, Ni YG, Hubbard B, Sitlani A and Carfi A. Mechanistic implications for LDL receptor degradation from the PCSK9/LDLR structure at neutral pH. EMBO Rep. 2011;12:1300–5. [PubMed: 22081141]
7. Ungewickell A, Hugge C, Kisseleva M, Chang SC, Zou J, Feng Y, Galyov EE, Wilson M and Majerus PW. The identification and characterization of two phosphatidylinositol-4,5-bisphosphate 4-phosphatases. Proc Natl Acad Sci U S A. 2005;102:18854–9. [PubMed: 16365287]
8. Tan X, Thapa N, Choi S and Anderson RA. Emerging roles of PtdIns(4,5)P2--beyond the plasma membrane. J Cell Sci. 2015;128:4047–56. [PubMed: 26574506]
9. Pryor PR, Mullock BM, Bright NA, Gray SR and Luzio JP. The role of intraorganellar Ca(2+) in late endosome-lysosome heterotypic fusion and in the reformation of lysosomes from hybrid organelles. J Cell Biol. 2000;149:1053–62. [PubMed: 10831609]
10. Yan H, Ma YL, Gui YZ, Wang SM, Wang XB, Gao F and Wang YP. MG132, a proteasome inhibitor, enhances LDL uptake in HepG2 cells in vitro by regulating LDLR and PCSK9 expression. Acta Pharmacol Sin. 2014;35:994–1004. [PubMed: 25042549]
11. Vicinanza M, Di Campli A, Polishchuk E, Santoro M, Di Tullio G, Godi A, Levtchenko E, De Leo MG, Polishchuk R, Sandoval L, Marzolo MP and De Matteis MA. OCRL controls trafficking through early endosomes via PtdIns4,5P(2)-dependent regulation of endosomal actin. EMBO J. 2011;30:4970–85. [PubMed: 21971085]
12. Ketel K, Krauss M, Nicot AS, Puchkov D, Wieffer M, Muller R, Subramanian D, Schultz C, Laporte J and Haucke V. A phosphoinositide conversion mechanism for exit from endosomes. Nature. 2016;529:408–12. [PubMed: 26760201]
13. Choi S, Thapa N, Tan X, Hedman AC and Anderson RA. PIP kinases define PI4,5P(2)signaling specificity by association with effectors. Biochim Biophys Acta. 2015;1851:711–23. [PubMed: 25617736]
14. Qin Y, Sundaram S, Essaid L, Chen X, Miller SM, Yan F, Darr DB, Galanko JA, Montgomery SA, Major MB, Johnson GL, Troester MA and Makowski L. Weight loss reduces basal-like breast cancer through kinome reprogramming. Cancer Cell Int. 2016;16:26. [PubMed: 27042159]
15. Chiu S, Bergeron N, Williams PT, Bray GA, Sutherland B and Krauss RM. Comparison of the DASH (Dietary Approaches to Stop Hypertension) diet and a higher-fat DASH diet on blood pressure and lipids and lipoproteins: a randomized controlled trial. Am J Clin Nutr. 2016;103:341–7. [PubMed: 26718414]
16. Musunuru K, Orho-Melander M, Caulfield MP, Li S, Salameh WA, Reitz RE, Berglund G, Hedblad B, Engstrom G, Williams PT, Kathiresan S, Melander O and Krauss RM. Ion mobility analysis of lipoprotein subfractions identifies three independent axes of cardiovascular risk. Arterioscler Thromb Vasc Biol. 2009;29:1975–80. [PubMed: 19729614]
17. Caulfield MP, Li S, Lee G, Blanche PJ, Salameh WA, Benner WH, Reitz RE and Krauss RM. Direct determination of lipoprotein particle sizes and concentrations by ion mobility analysis. Clin Chem. 2008;54:1307–16. [PubMed: 18515257]
18. Sun H, Samarghandi A, Zhang N, Yao Z, Xiong M and Teng BB. Proprotein convertase subtilisin/kexin type 9 interacts with apolipoprotein B and prevents its intracellular degradation, irrespective of the low-density lipoprotein receptor. Arterioscler Thromb Vasc Biol. 2012;32:1585–95. [PubMed: 22580899]
19. Johnson AR, Qin Y, Cozzo AJ, Freemerman AJ, Huang MJ, Zhao L, Sampey BP, Milner JJ, Beck MA, Damania B, Rashid N, Galanko JA, Lee DP, Edin ML, Zeldin DC, Fueger PT, Dietz B, Stahl A, Wu Y, Mohlke KL and Makowski L. Metabolic reprogramming through fatty acid transport protein 1 (FATP1) regulates macrophage inflammatory potential and adipose inflammation. Mol Metab. 2016;5:506–526. [PubMed: 27408776]
20. Folch J, Lees M and Sloane Stanley GH. A simple method for the isolation and purification of total lipides from animal tissues. J Biol Chem. 1957;226:497–509. [PubMed: 13428781]
21. Gulshan K, Brubaker G, Conger H, Wang S, Zhang R, Hazen SL and Smith JD. PI(4,5)P2 Is Translocated by ABCA1 to the Cell Surface Where It Mediates Apolipoprotein A1 Binding and Nascent HDL Assembly. Circ Res. 2016;119:827–38. [PubMed: 27514935]

22. Moldeus P, Hogberg J and Orrenius S. Isolation and use of liver cells. Methods Enzymol. 1978;52:60–71. [PubMed: 672656]

23. Hashimoto Y, Shirane M and Nakayama KI. TMEM55B contributes to lysosomal homeostasis and amino acid-induced mTORC1 activation. Genes Cells. 2018;23:418–434. [PubMed: 29644770]

24. Jang MK and Jung MH. ATF3 inhibits PPARgamma-stimulated transactivation in adipocyte cells. Biochem Biophys Res Commun. 2015;456:80–5. [PubMed: 25446101]

25. Bell TA 3rd, Brown JM, Graham MJ, Lemonidis KM, Crooke RM and Rudel LL. Liver-specific inhibition of acyl-coenzyme a:cholesterol acyltransferase 2 with antisense oligonucleotides limits atherosclerosis development in apolipoprotein B100-only low-density lipoprotein receptor−/− mice. Arterioscler Thromb Vasc Biol. 2006;26:1814–20. [PubMed: 16675724]

26. Warnick GR, Nguyen T and Albers AA. Comparison of improved precipitation methods for quantification of high-density lipoprotein cholesterol. Clin Chem. 1985;31:217–22. [PubMed: 2578337]

27. Tavori H, Rashid S and Fazio S. On the function and homeostasis of PCSK9: reciprocal interaction with LDLR and additional lipid effects. Atherosclerosis. 2015;238:264–70. [PubMed: 25544176]

28. Willett R, Martina JA, Zewe JP, Wills R, Hammond GRV and Puertollano R. TFEB regulates lysosomal positioning by modulating TMEM55B expression and JIP4 recruitment to lysosomes. Nat Commun. 2017;8:1580. [PubMed: 29146937]

29. Maxfield FR and McGraw TE. Endocytic recycling. Nat Rev Mol Cell Biol. 2004;5:121–32. [PubMed: 15040445]

30. Mishra SK, Keyel PA, Edeling MA, Dupin AL, Owen DJ and Traub LM. Functional dissection of an AP-2 beta2 appendage-binding sequence within the autosomal recessive hypercholesterolemia protein. J Biol Chem. 2005;280:19270–80. [PubMed: 15728179]

31. Johnson DE, Ostrowski P, Jaumouille V and Grinstein S. The position of lysosomes within the cell determines their luminal pH. J Cell Biol. 2016;212:677–92. [PubMed: 26975849]

32. Pu J, Guardia CM, Keren-Kaplan T and Bonifacino JS. Mechanisms and functions of lysosome positioning. J Cell Sci. 2016;129:4329–4339. [PubMed: 27799357]

33. Misinzo G, Delputte PL and Nauwynck HJ. Inhibition of endosome-lysosome system acidification enhances porcine circovirus 2 infection of porcine epithelial cells. J Virol. 2008;82:1128–35. [PubMed: 18032516]

34. Bartuzi P, Billadeau DD, Favier R, Rong S, Dekker D, Fedoseienko A, Fieten H, Wijers M, Levels JH, Huijkman N, Kloosterhuis N, van der Molen H, Brufau G, Groen AK, Elliott AM, Kuivenhoven JA, Plecko B, Grangl G, McGaughran J, Horton JD, Burstein E, Hofker MH and van de Sluis B. CCC- and WASH-mediated endosomal sorting of LDLR is required for normal clearance of circulating LDL. Nat Commun. 2016;7:10961. [PubMed: 26965651]

35. Hong C, Marshall SM, McDaniel AL, Graham M, Layne JD, Cai L, Scotti E, Boyadjian R, Kim J, Chamberlain BT, Tangirala RK, Jung ME, Fong L, Lee R, Young SG, Temel RE and Tontonoz P. The LXR-Idol axis differentially regulates plasma LDL levels in primates and mice. Cell Metab. 2014;20:910–918. [PubMed: 25440061]

36. De Leo MG, Staiano L, Vicinanza M, Luciani A, Carissimo A, Mutarelli M, Di Campli A, Polishchuk E, Di Tullio G, Morra V, Levtchenko E, Oltrabella F, Starborg T, Santoro M, di Bernardo D, Devuyst O, Lowe M, Medina DL, Ballabio A and De Matteis MA. Autophagosome-lysosome fusion triggers a lysosomal response mediated by TLR9 and controlled by OCRL. Nat Cell Biol. 2016;18:839–50. [PubMed: 27398910]

37. Festa BP, Berquez M, Gassama A, Amrein I, Ismail HM, Samardzija M, Staiano L, Luciani A, Grimm C, Nussbaum RL, De Matteis MA, Dorchies OM, Scapozza L, Wolfer DP and Devuyst O. OCRL deficiency impairs endolysosomal function in a humanized mouse model for Lowe syndrome and Dent disease. Hum Mol Genet. 2019;28:1931–1946. [PubMed: 30590522]

38. Zolov SN, Bridges D, Zhang Y, Lee WW, Riehle E, Verma R, Lenk GM, Converso-Baran K, Weide T, Albin RL, Saltiel AR, Meisler MH, Russell MW and Weisman LS. In vivo, Pikfyve generates PI(3,5)P2, which serves as both a signaling lipid and the major precursor for PI5P. Proc Natl Acad Sci U S A. 2012;109:17472–7. [PubMed: 23047693]

39. Ikonomov OC, Sbrissa D, Delvecchio K, Xie Y, Jin JP, Rappolee D and Shisheva A. The phosphoinositide kinase PIKfyve is vital in early embryonic development: preimplantation

lethality of PIKfyve−/− embryos but normality of PIKfyve+/− mice. J Biol Chem. 2011;286:13404–13. [PubMed: 21349843]

40. Hu A, Zhao XT, Tu H, Xiao T, Fu T, Wang Y, Liu Y, Shi XJ, Luo J and Song BL. PIP4K2A regulates intracellular cholesterol transport through modulating PI(4,5)P2 homeostasis. J Lipid Res. 2018;59:507–514. [PubMed: 29353240]
41. Woollett LA, Osono Y, Herz J and Dietschy JM. Apolipoprotein E competitively inhibits receptor-dependent low density lipoprotein uptake by the liver but has no effect on cholesterol absorption or synthesis in the mouse. Proc Natl Acad Sci U S A. 1995;92:12500–4. [PubMed: 8618929]
42. Blasiole DA, Oler AT and Attie AD. Regulation of ApoB secretion by the low density lipoprotein receptor requires exit from the endoplasmic reticulum and interaction with ApoE or ApoB. J Biol Chem. 2008;283:11374–81. [PubMed: 18272520]
43. Nassir F, Xie Y, Patterson BW, Luo J and Davidson NO. Hepatic secretion of small lipoprotein particles in apobec-1−/− mice is regulated by the LDL receptor. J Lipid Res. 2004;45:1649–59. [PubMed: 15145984]
44. Bierwolf J, Lutgehetmann M, Feng K, Erbes J, Deichmann S, Toronyi E, Stieglitz C, Nashan B, Ma PX and Pollok JM. Primary rat hepatocyte culture on 3D nanofibrous polymer scaffolds for toxicology and pharmaceutical research. Biotechnol Bioeng. 2011;108:141–50. [PubMed: 20824672]
45. Yamamoto T, Davis CG, Brown MS, Schneider WJ, Casey ML, Goldstein JL and Russell DW. The human LDL receptor: a cysteine-rich protein with multiple Alu sequences in its mRNA. Cell. 1984;39:27–38. [PubMed: 6091915]
46. Goldstein JL and Brown MS. The LDL receptor. Arterioscler Thromb Vasc Biol. 2009;29:431–8. [PubMed: 19299327]
47. Korolchuk VI, Saiki S, Lichtenberg M, Siddiqi FH, Roberts EA, Imarisio S, Jahreiss L, Sarkar S, Futter M, Menzies FM, O'Kane CJ, Deretic V and Rubinsztein DC. Lysosomal positioning coordinates cellular nutrient responses. Nat Cell Biol. 2011;13:453–60. [PubMed: 21394080]
48. Pous C and Codogno P. Lysosome positioning coordinates mTORC1 activity and autophagy. Nat Cell Biol. 2011;13:342–4. [PubMed: 21460804]
49. Herz J and Strickland DK. LRP: a multifunctional scavenger and signaling receptor. J Clin Invest. 2001;108:779–84. [PubMed: 11560943]
50. Hammond GR, Machner MP and Balla T. A novel probe for phosphatidylinositol 4-phosphate reveals multiple pools beyond the Golgi. J Cell Biol. 2014;205:113–26. [PubMed: 24711504]
51. Sridhar S, Patel B, Aphkhazava D, Macian F, Santambrogio L, Shields D and Cuervo AM. The lipid kinase PI4KIIIbeta preserves lysosomal identity. EMBO J. 2013;32:324–39. [PubMed: 23258225]
52. Rong Y, Liu M, Ma L, Du W, Zhang H, Tian Y, Cao Z, Li Y, Ren H, Zhang C, Li L, Chen S, Xi J and Yu L. Clathrin and phosphatidylinositol-4,5-bisphosphate regulate autophagic lysosome reformation. Nat Cell Biol. 2012;14:924–34. [PubMed: 22885770]
53. Prabakaran S, Lippens G, Steen H and Gunawardena J. Post-translational modification: nature's escape from genetic imprisonment and the basis for dynamic information encoding. Wiley Interdiscip Rev Syst Biol Med. 2012;4:565–83. [PubMed: 22899623]

HIGHLIGHTS:

- *Tmem55b* regulates plasma non-HDL cholesterol levels *in vivo*.
- *TMEM55B* knockdown decreases LDLR levels through increasing LDLR partitioning to lysosomes.
- *TMEM55B* regulates cellular LDLR lysosomal decay and recycling through $PI(4,5)P_2$

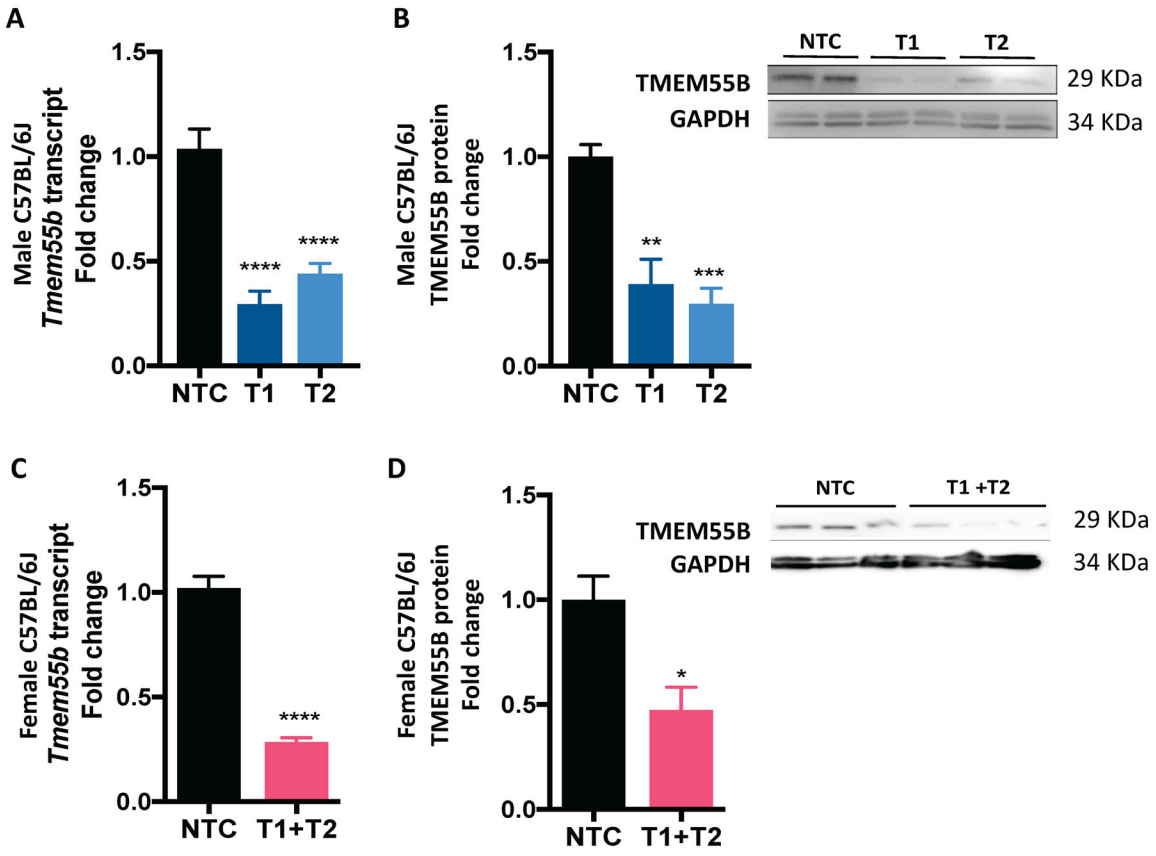

Figure 1.

Tmem55b knockdown with antisense oligonucleotides (ASO). Six-week old male (**A**,**B**) and female (**C**,**D**) C57BL/6J mice were treated with an ASO against *Tmem55b* (T1, T2 or T1+T2) or a non-targeting control (NTC) at a dose of 25 mg/kg body weight/week and fed a Western diet (0.2% cholesterol, 42% fat) for 4 weeks. Hepatic *Tmem55b* transcript (**A**, **C**) was detected by qPCR (mean ± s.e.m. of the fold change from NTC treated animals) with values normalized to *Clptm*. Protein (**B**, **D**) levels were detected by immunoblot. Quantified results are presented as mean ± s.e.m. N=9–10 in male mice; N=6–8 in female mice. **p<0.01, ***p<0.001, ****p<0.0001 vs. NTC by one-way ANOVA or Student's t-test.

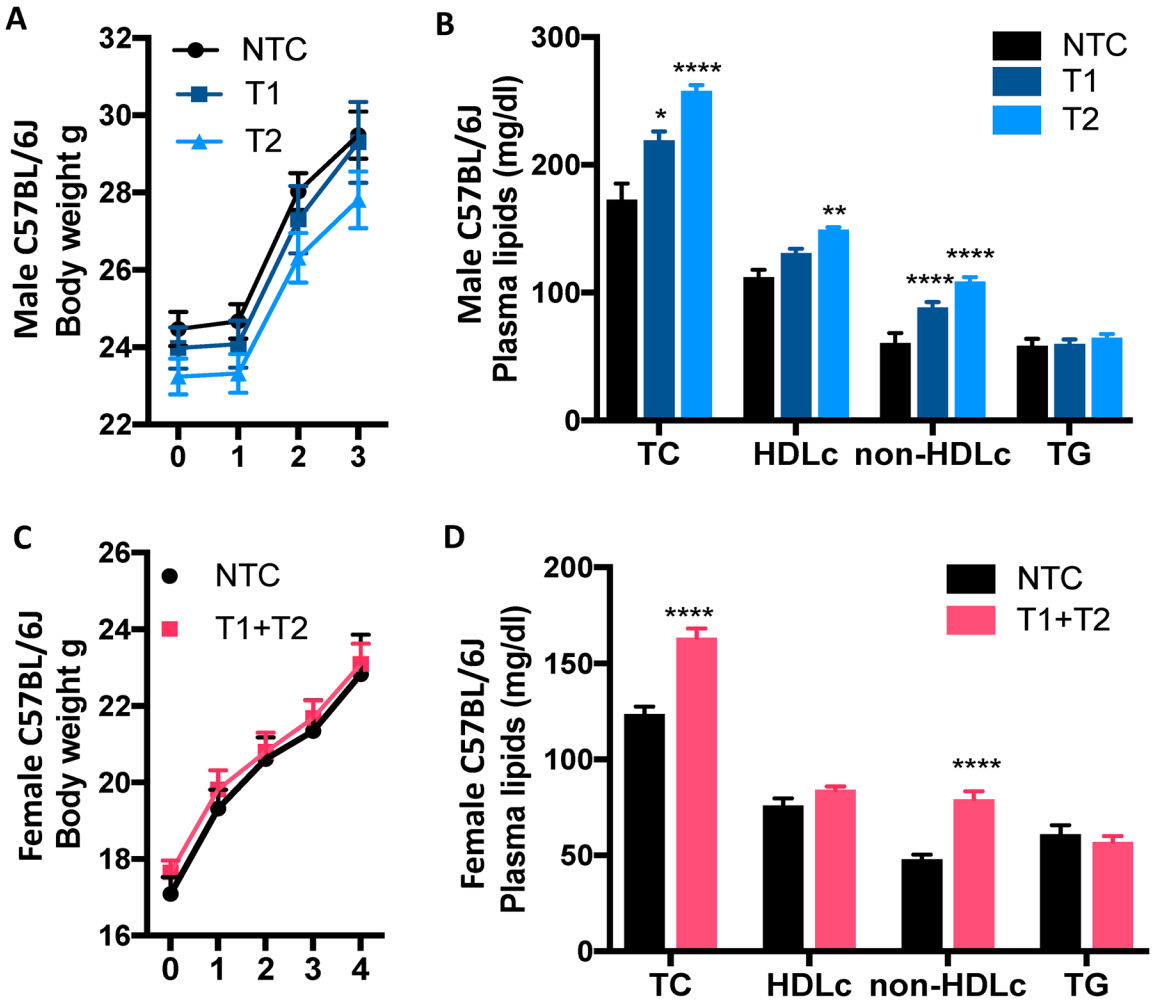

Figure 2.

Tmem55b knockdown increases plasma cholesterol. Body weight of male (**A**) and female (**C**) mice was measured weekly before and 3–4 weeks after ASO (*Tmem55b* T1 and/or T2, or NTC) and Western diet treatment. Plasma TC, HDLc and TG from male (**B**) and female (**D**) mice were quantified with AMS Liasys 330 Clinical Chemistry Analyzer, and LDLc was calculated by subtraction of HDLc from TC. N=9–10 in male mice; N=6–8 in female mice. Numeric data represent the means ± s.e.m. *p<0.05, **p<0.01, ****p<0.0001 vs. NTC by one-way ANOVA or Student's t-test.

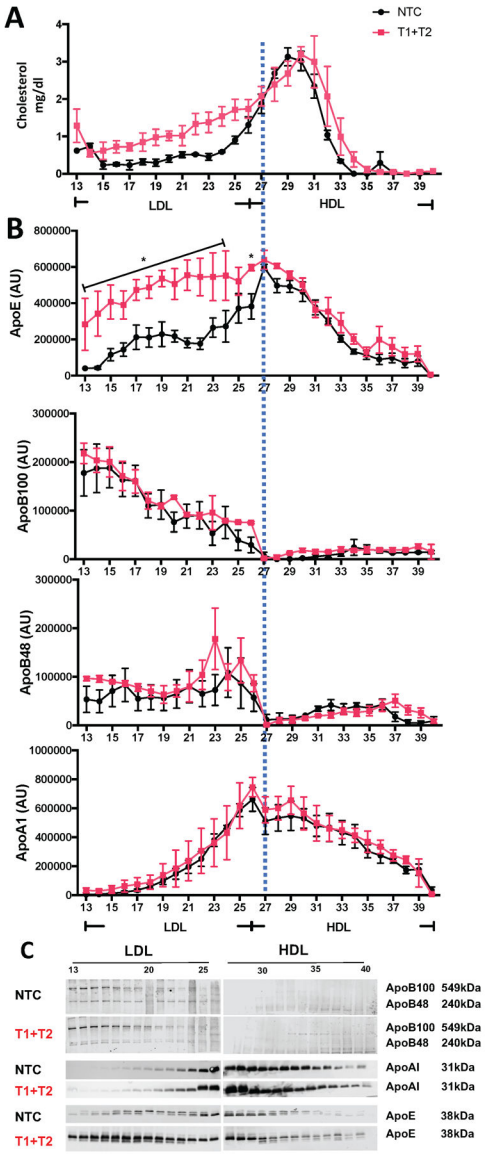

Figure 3.

Tmem55b knockdown increases plasma cholesterol on apoE containing particles. Pooled plasma from female mice (n=3/treatment, with each plasma sample pooled from 2 littermate mice) was separated by FPLC. Total cholesterol (**A**) and apolipoproteins B100, B48, E and A1 (**B**) in each FPLC plasma fraction were quantified with enzymatic assay or Western blot (n=3). (**C**). Representative images of B. *p<0.05 vs. NTC by Student's t-test.

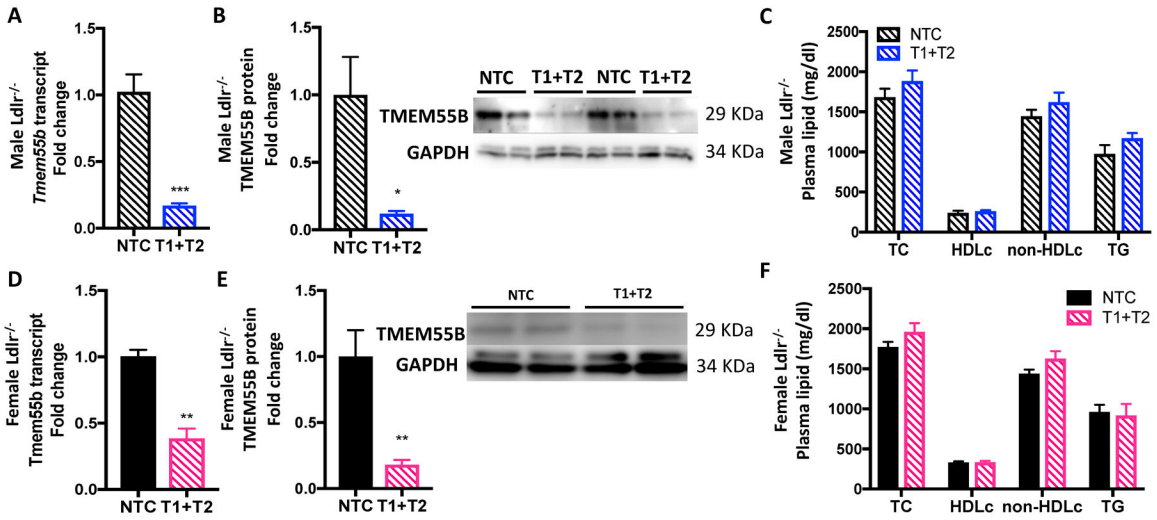

Figure 4.

Tmem55b does not alter plasma lipids in *Ldlr*$^{-/-}$ mice. Six-week old *Ldlr*$^{-/-}$ male (**A**,**B**,**C**) and female (**D**,**E**,F) mice (n=4 per sex per group) were fed Western diet and treated with NTC or *Tmem55b* ASO (T1+T2) weekly for 4 weeks. Hepatic *Tmem55b* transcript (**A**, **D**) and protein (**B**, **E**) levels were detected by qPCR and immunoblot, respectively. (**C**,**F**) TC, HDLc and TG were quantified with AMS Liasys 330 Clinical Chemistry Analyzer, and LDLc was calculated by subtraction of HDLc from TC. Numeric data represent the means ± s.e.m. *p<0.05, **p<0.01 vs. NTC by Student's t-test.

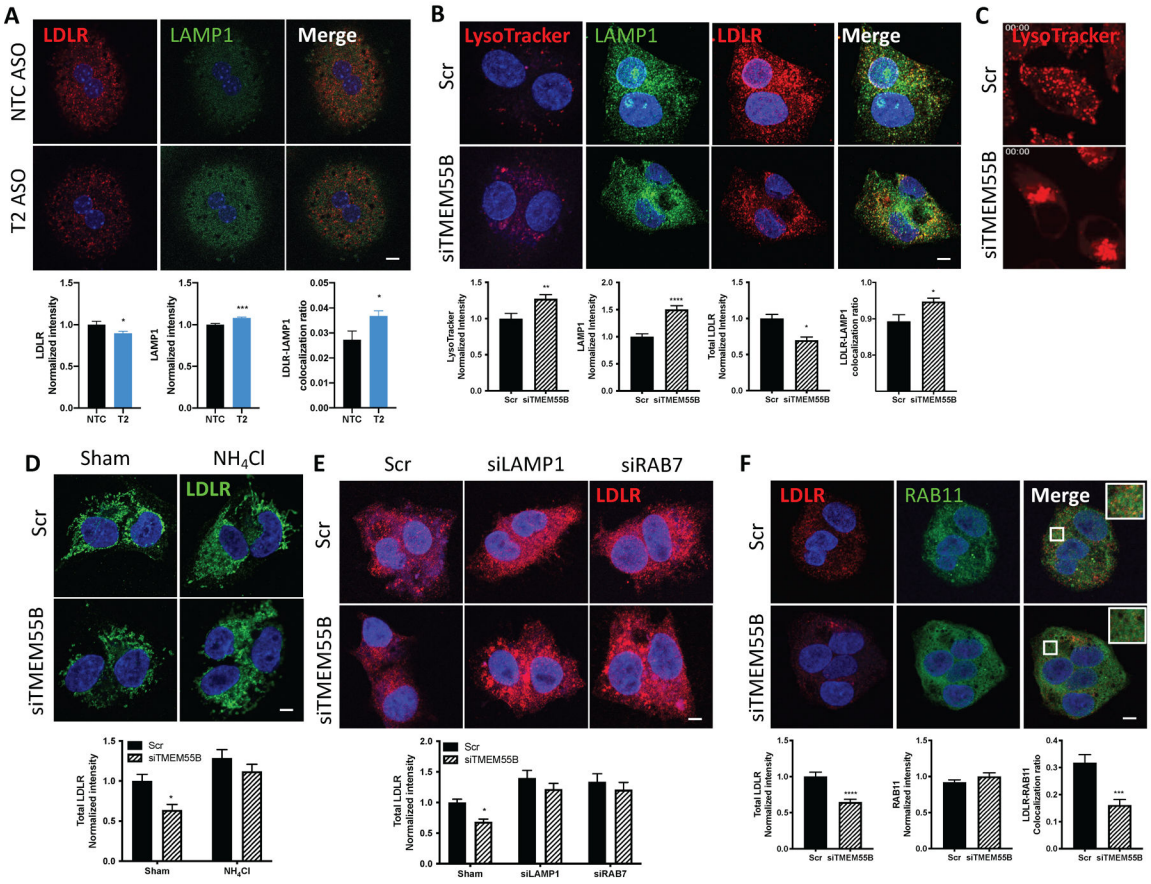

Figure 5.

Tmem55b knockdown increases LDLR-lysosomal degradation and reduces LDLR recycling. Primary hepatocytes were isolated from NTC and T2 ASO treated 8-week-old male mice. HepG2 or McArdle cells were transfected with siRNAs targeting *TMEM55B* (siTMEM) or a scrambled control (Scr) for 36 hours. (**A**) Primary hepatocytes were stained with antibodies against LDLR and/or LAMP1 at 4°C overnight, and examined by confocal microscopy. (**B**) Permeabilized HepG2 cells were incubated with LysoTracker for 2 hours or stained with antibodies against LDLR and/or LAMP1 at 4°C, and examined by confocal microscopy. (**C**) McArdle cells were treated with oleic acid for 45 min and incubated with LysoTracker for 2 hours. (**D**) 12 hours after siRNA transfection, HepG2 cells were treated with either 10 mM NH_4Cl or sham buffer, and LDLR was visualized after 24 hr with anti-LDLR. (**E**) HepG2 cells were transfected with siRNAs targeting *TMEM55B* with and without *LAMP1* and *RAB7* or Scr control, and LDLR was visualized after 36 hours. (**F**) siRNA treated HepG2 cells were incubated with antibodies against LDLR and RAB11. Representative images are shown. Quantification was performed using 15–35 randomly chosen fields that included 1–5 cells each, with images analyzed using the Carl Zeiss software, and representative images are shown. Colocalization was quantified with Carl Zeiss software AIM using Pearson's Correlation Coefficients. Numeric data represent mean ± s.e.m. *p<0.05, **p<0.01, ***p<0.001, ****p<0.0001 vs. NTC or Scr by Student's t-test. Scale bars, 10 μm.

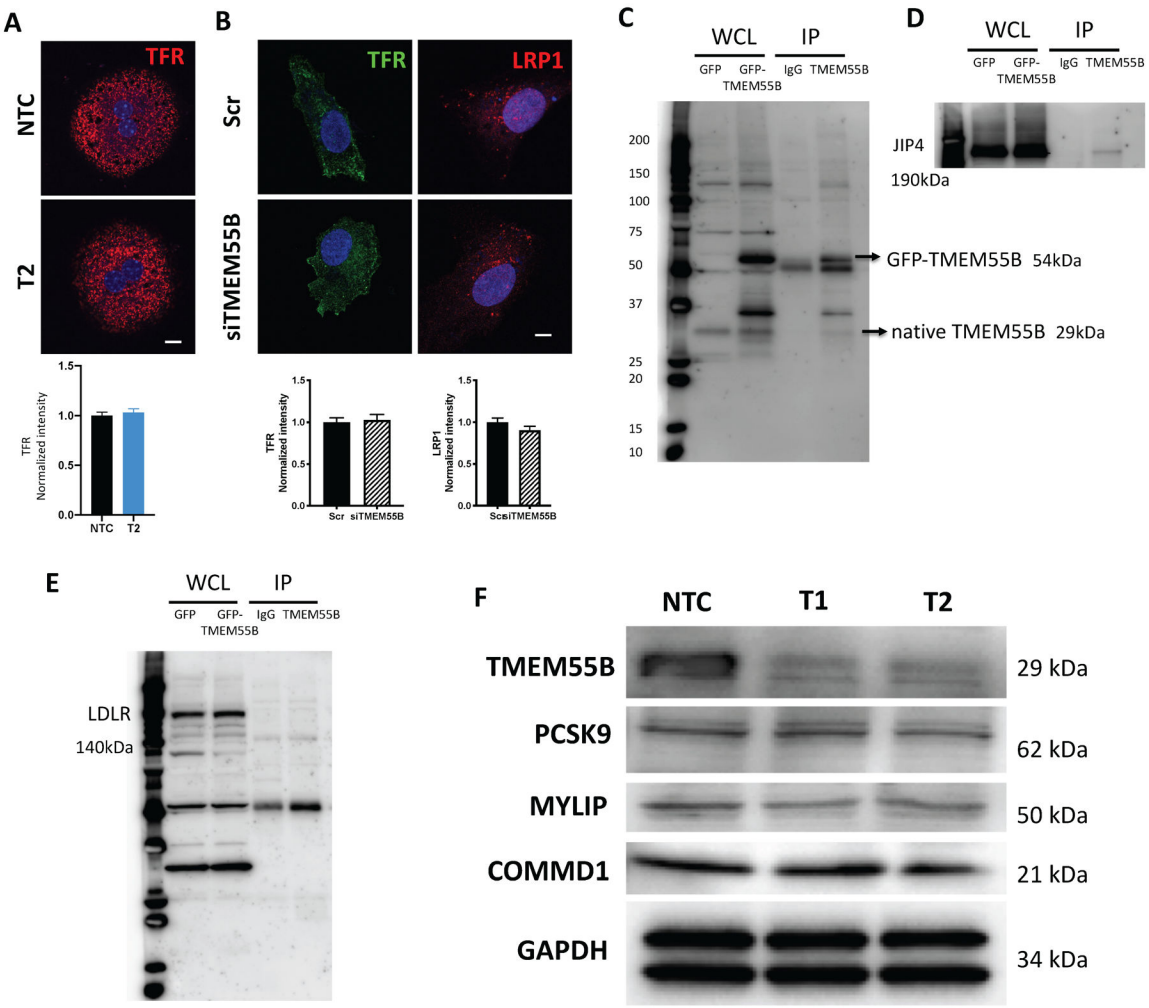

Figure 6.

TMEM55B does not regulate recycling receptors in general, and does not bind LDLR. (**A**) Primary hepatocytes were isolated from NTC and T2 ASO treated 8-week-old male mice, stained with anti-transferrin receptor antibody at 4°C overnight, and examined by confocal microscopy. (**B**) HepG2 cells were transfected with siRNAs targeting *TMEM55B* (siTMEM) or a scrambled control (Scr) for 36 hr. Cells were incubated with 1° antibodies against TFR and/or LRP1 at 4°C, and examined by confocal microscopy. Representative images are shown. Quantification was performed as described in Figure 1. *p<0.05 vs. Scr by Student's t-test. Scale bars, 10 μm. (**C**-**E**) HepG2 cells were transfected with *TMEM55B-GFP* over-expression (GFP-TMEM) or GFP (negative control) plasmids for 48 hr, then cells were lysed and subjected to co-immunoprecipitation (IP) with anti-TMEM55B antibody or an IgG negative control. The resulting precipitates, as well as a portion of the whole cell lysate (WCL), were subjected to immunoblotting with anti-TMEM55B, Anti-JIP4, and anti-LDLR antibodies. Experiments were repeated 3 times, with representative images shown. (**F**) Images of western blot results for TMEM55B, PCSK9, MYLIP/IDOL, and COMMD1 from liver lysates of NTC, T1, and T2 treated male mice. GAPDH was used as internal control (n=4). Experiments were repeated 3 times with representative images shown.

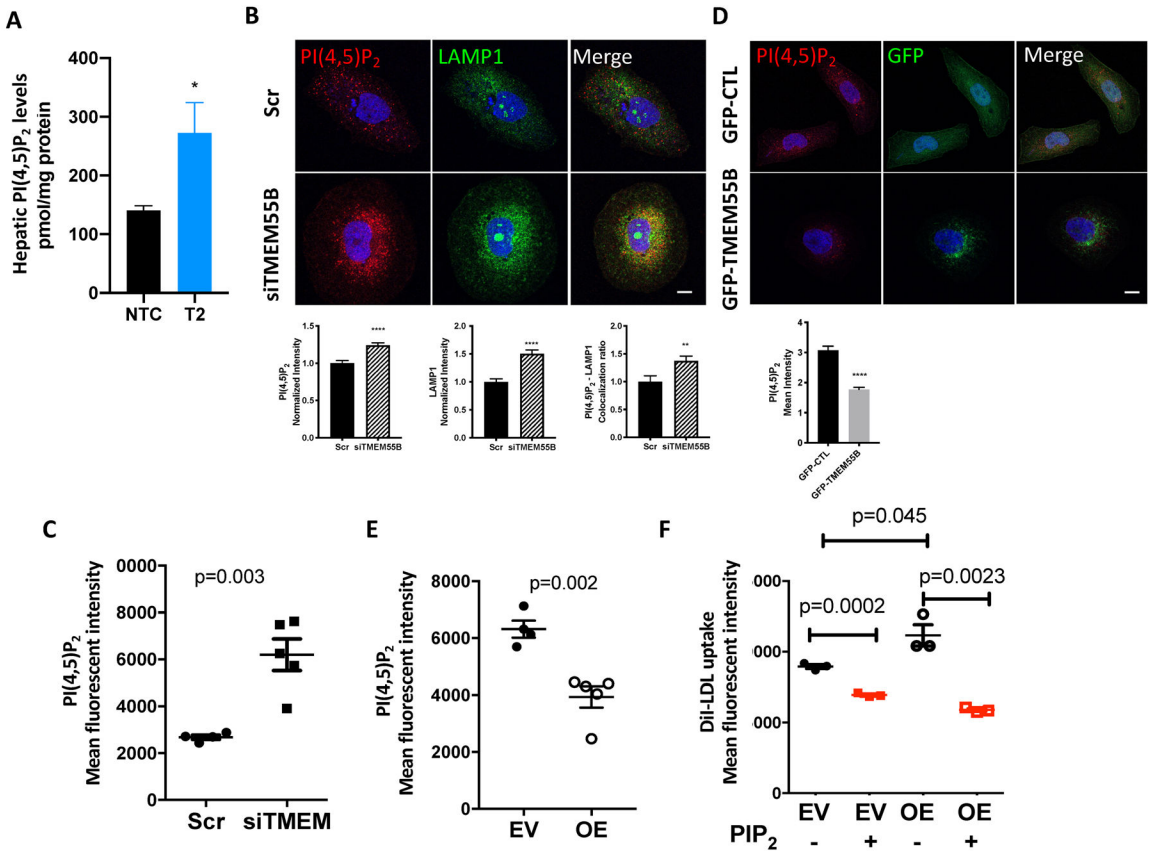

Figure 7.

TMEM55B regulates LDL uptake through PI(4,5)P_2. (**A**) PI(4,5)P_2 levels from liver lysates of NTC- and T2-ASO treated male mice were assessed (n=6–7). HepG2 cells (n=5–8) were transfected with siRNAs targeting *TMEM55B* (siTMEM) or a scrambled control (Scr) for 36 hours (**B**, **C**), or with *TMEM55B* over-expression (OE) or empty-vector (EV) plasmids for 48hr (**D**, **E**). Cells were then permeabilized, and incubated with an antibody against PI(4,5)P_2 or Lamp1 at 4°C overnight, and examined by confocal microscopy (**B**, **D**) or BD FACS Calibur (**C**, **E**). (**F**) HepG2 cells (n=3) were first transfected with *TMEM55B* OE or EV plasmids for 48hr and incubated with PI(4,5)P_2 or control liposomes without any no PIPn from Echelon Bioscience. Then all cells were incubated with 10ug/ml Dil-labeled LDL for 3 hr at 37°C. Dil fluorescence was quantified on the BD FACS Calibur as the median fluorescence values of 10,000 gated events. For confocal microscopy, quantification was performed using 30–35 randomly chosen fields that included 1–5 cells each, with images analyzed using Carl Zeiss software, and representative images are shown. Colocalization was quantified with Carl Zeiss software AIM using Pearson's Correlation Coefficients. Numeric data represent means ± s.e.m. **p<0.01, ****p<0.0001 vs. NTC by Student's t-test. Scale bars, 10 μm.